On the Simulation of Plasma Waves in HEMTs and the Dyakonov-Shur Instability

1st Christoph Jungemann
Chair of Electromagnetic Theory
RWTH Aachen University
Aachen, Germany
cj@ithe.rwth-aachen.de

2nd Tobias Linn
Chair of Electromagnetic Theory
RWTH Aachen University
Aachen, Germany
tl@ithe.rwth-aachen.de

3rd Zeinab Kargar
Chair of Electromagnetic Theory
RWTH Aachen University
Aachen, Germany
zk@ithe.rwth-aachen.de

***Abstract*—Modeling of plasma waves in HEMTs by moments-based transport models is investigated. The balance equations are derived from the Boltzmann transport equation by projection onto Hermitian polynomials. The discretized equations are stabilized by an approach based on matrix exponentials, which in the case of the drift-diffusion model reproduces the Scharfetter-Gummel stabilization. Simulations of a realistic HEMT show that plasma instabilities are rather unlikely to occur and that effects not considered by Dyakonov and Shur (e.g. real ohmic contacts) strongly damp the THz waves. Furthermore, quasi-ballistic transport can not be captured by higher-order models.**

***Index Terms*—HEMT, plasma waves, drift-diffusion, Boltzmann transport equation, Scharfetter-Gummel stabilization**

I. Introduction

Many promising high-frequency applications fall into the so-called THz gap (0.3-3THz), for which only very power-inefficient sources exist [1]. Dyakonov and Shur proposed THz wave sources based on plasma instabilities in high electron mobility transistors (HEMT), which might fill this gap [2], [3]. Due to an applied dc drain/source bias a current flows in the channel and the plasma waves in the direction of the electron flow (downstream) behave differently from the plasma waves in the opposite direction (upstream). They assumed that the ac electron density at the source-side of the channel is zero and that the ac electron current at the drain-side vanishes. These boundary conditions can lead to a plasma instability and the generation of THz waves. For a HEMT in the common source configuration these boundary conditions correspond to an ac-shorted gate/source (input) port and open drain/source (output) port. Since HEMTs with a negative differential output resistance are in general not unconditionally stable, such a configuration almost always leads to oscillations at rather low frequencies [4]. Experimental verification of THz wave generation by plasma instabilities is therefore difficult and the experimental results are rather inconclusive. Furthermore, the measured THz emissions are often barely above the black body radiation (e.g. [5]). It is thus not clear whether plasma instabilities can be used to generate THz waves or not and in this paper we investigate the accuracy of the underlying theory by device simulation.

Financial support by the German Science Foundation (DFG) under contract number JU406/14-1 is gratefully acknowledged.

II. Model

The hydrodynamic modeling approach used by Dyakonov and Shur is questionable for various reasons. Their model based on the Euler and continuity equations is similar to a drift-diffusion model which includes the convective derivative and a time derivative in the constitutive equation for the electron current density [6]. It can be derived from the Boltzmann transport equation (BTE) by taking the first two (velocity) moments together with a closure relation based on a drifted Maxwellian [7], [8]. This assumption holds only in the case of strong scattering, whereas THz wave generation requires extremely high mobilities and thus quasi-ballistic transport [2], [3]. A quasi-ballistic distribution function in a device is very different from a Maxwellian in the case of nonequilibrium and it is not clear whether electron-electron scattering is sufficiently strong to drive the distribution function towards a Maxwellian on the required time and length scales. In addition, the Maxwellian will be heated, a fact that was neglected by Dyakonov and Shur and leads to a strong increase of the channel resistance and damping of the plasma instability, especially at high mobilities [9]. Moreover, the restriction to two moments leads to a plasma dispersion relation with only two branches, whereas the BTE yields in addition a continuum of modes [10]. In order to capture the impact of the additional modes, the differential equations should be solved in the real space, which also allows to account for inhomogeneous channels and parasitics. In addition, it is possible to apply more realistic boundary conditions. The assumption of a drift-diffusion model together with Dirichlet boundary conditions at the source and drain terminals leads for high mobilities to unrealistically large conductivities, which exceed the ballistic limit for thermal bath boundary conditions. This can be at least partially avoided by assuming a finite surface recombination velocity (real ohmic contacts) [11].

In order to avoid some of the above mentioned problems, we solve moments-based models of arbitrary order l for a realistic 2D device structure (Fig. 1). While the Poisson equation for the quasi-stationary potential is solved in 2D, the electron transport for the electron gas in the channel is assumed to be 1D (charge sheet approximation) [12]. The Poisson equation is discretized by the finite volume method in conjunction

978-1-7281-0940-4/19/$31.00 © 2019 IEEE

with finite differences for the electric flux density [11]. On the contacts Dirichlet boundary conditions are applied to the potential, otherwise homogeneous Neumann boundary conditions. The 1D transport models are derived from the BTE by projection onto Hermitian polynomials assuming a macroscopic relaxation time approximation for the scattering integral and a parabolic band structure:

$$\frac{\partial g_n}{\partial t}+\frac{2neE_x}{\sqrt{2mk_\mathrm{B}T_0}}g_{n-1}+\sqrt{\frac{2k_\mathrm{B}T_0}{m}}\left(\frac{1}{2}\frac{\partial g_{n+1}}{\partial x}+n\frac{\partial g_{n-1}}{\partial x}\right)=-\frac{g_n-g_0\delta_{n,0}}{\tau} \tag{1}$$

e is the elementary charge, $E_x(x,t)$ is the x component of the electric field in the channel, m the effective mass, $k_\mathrm{B}T_0$ the thermal energy and τ the macroscopic relaxation time with $\mu = e\tau/m$. For the sake of simplicity τ is assumed to be position independent. $g_n(x,t)$ is the nth moment of the distribution function,

$$f(x,\vec{k},t)=\sum_{n=0}^{\infty}\frac{g_n(x,t)H_n\left(\frac{\hbar k_x}{\sqrt{2mk_\mathrm{B}T_0}}\right)}{2^n n!\sqrt{\pi}}\mathrm{e}^{-\frac{\hbar^2\vec{k}^2}{2mk_\mathrm{B}T_0}} \tag{2}$$

where $H_n(u)$ is the nth order Hermitian polynomial [13]. This special type of distribution function is due to the assumption of 1D transport in the real space and the macroscopic relaxation time approximation for the scattering integral. The electron density is proportional to the zeroth order component: $n(x,t) = N_\mathrm{C}/\sqrt{\pi}\ g_0(x,t)$, and the electron current density is given by: $j_x(x,t) = N_\mathrm{C}\sqrt{k_\mathrm{B}T_0}/\sqrt{2m\pi}\ g_1(x,t)$, where N_C is the effective density of states of the conduction band. The terminal currents are evaluated by the extended Ramo-Shockley theorem [14].

In order to obtain a system of equations of finite size, the expansion in (2) is truncated at maximum order l and all components for $n > l$ are assumed to be zero ($g_{n>l}(x,t) = 0$). This closure relation has the advantage that the equations remain linear, but it can lead to stability problems for large electric fields. For $l = 1$ the drift-diffusion model is obtained without the convective derivative. To account for such transport effects in a more rigorous manner, transport models with a much larger l are solved (e.g. $l = 9$), where the convergence of the expansion must be checked.

For a finite l the balance equations (1) for different n can be aggregated into:

$$\frac{\partial\vec{g}}{\partial t}+\hat{A}\frac{\partial\vec{g}}{\partial x}+\hat{B}\vec{g}=\vec{0} \tag{3}$$

$\vec{g}(x,t)$ is the vector containing the l components. $\hat{A}$ is a constant $l\times l$ matrix and $\hat{B}$ depends on the electric field. A grid with N nodes x_i is used for the channel. First, the dc case is considered, for which (3) can be solved under the assumption of a position independent $\hat{C}_{i+\frac{1}{2}} = \hat{A}^{-1}\hat{B}_{i+\frac{1}{2}}$ in the interval $[x_i, x_{i+1}]$ with the matrix exponential [15], where $\vec{G}_i = \vec{G}(x_i)$ is the dc solution, $x_{i+\frac{1}{2}} = (x_{i+1}+x_i)/2$ and $\hat{D}_{i+\frac{1}{2}}(x) = -\hat{C}_{i+\frac{1}{2}}(x - x_{i+\frac{1}{2}})$:

$$\vec{G}(x)=\mathrm{e}^{\hat{D}_{i+\frac{1}{2}}(x)}\vec{G}_{i+\frac{1}{2}} \tag{4}$$

The vector $\vec{G}$ is split into even and odd components with $\vec{G} = (\vec{G}_\mathrm{e}^\mathrm{T}, \vec{G}_\mathrm{o}^\mathrm{T})^\mathrm{T}$ and the even components on the grid points are given by:

$$\begin{pmatrix}\vec{G}_{\mathrm{e},i}\\ \vec{G}_{\mathrm{e},i+1}\end{pmatrix}=\begin{pmatrix}\hat{P}\mathrm{e}^{\hat{D}_{i+\frac{1}{2}}(x_i)}\\ \hat{P}\mathrm{e}^{\hat{D}_{i+\frac{1}{2}}(x_{i+1})}\end{pmatrix}\vec{G}_{i+\frac{1}{2}}=\hat{H}_{i+\frac{1}{2}}\vec{G}_{i+\frac{1}{2}} \tag{5}$$

$\hat{P}$ is a nonsquare matrix selecting the even components: $\vec{G}_\mathrm{e} = \hat{P}\vec{G}$. On the grid nodes the fluxes must be continuous:

$$\hat{P}\hat{A}\mathrm{e}^{\hat{D}_{i-\frac{1}{2}}(x_i)}\hat{H}^{-1}_{i-\frac{1}{2}}\begin{pmatrix}\vec{G}_{\mathrm{e},i-1}\\ \vec{G}_{\mathrm{e},i}\end{pmatrix}=\hat{P}\hat{A}\mathrm{e}^{\hat{D}_{i+\frac{1}{2}}(x_i)}\hat{H}^{-1}_{i+\frac{1}{2}}\begin{pmatrix}\vec{G}_{\mathrm{e},i}\\ \vec{G}_{\mathrm{e},i+1}\end{pmatrix} \tag{6}$$

This equation links the even components on the nodes $i-1$, i and $i+1$. For $l = 1$ the well known Scharfetter-Gummel stabilization is obtained [16]. On the contacts a constant surface recombination velocity is used. At the source this yields:

$$-\left(\vec{G}_{\mathrm{e},1}-\vec{G}_{\mathrm{e,eq}}\right)v_\mathrm{s}=\hat{P}\hat{A}\mathrm{e}^{\hat{D}_{\frac{3}{2}}(x_1)}\hat{H}^{-1}_{\frac{3}{2}}\begin{pmatrix}\vec{G}_{\mathrm{e},1}\\ \vec{G}_{\mathrm{e},2}\end{pmatrix} \tag{7}$$

$\vec{G}_\mathrm{e,eq}$ is the equilibrium solution and v_s the surface recombination velocity. With a corresponding boundary condition for the drain a closed system of equations is obtained for the even components, which can be solved self-consistently with the Poisson equation by a Newton-Raphson method, where the electron density for the Poisson equation is evaluated on the grid nodes.

Small-signal analysis for the sinusoidal steady state condition is straightforward. Equation (3) is linearized with $\vec{g}(x,t) = \vec{G}(x) + \Re\left\{\underline{\vec{g}}(x)\mathrm{e}^{\mathrm{i}\omega t}\right\}$ and an expression for the complex phasors $\underline{\vec{g}}$, $\underline{E}_x$ is obtained:

$$\mathrm{i}\omega\underline{\vec{g}}+\hat{A}\frac{\partial\underline{\vec{g}}}{\partial x}+\hat{B}\underline{\vec{g}}=-\frac{\partial\hat{B}}{\partial E_x}\vec{G}\underline{E}_x \tag{8}$$

With $\underline{\hat{C}}'_{i+\frac{1}{2}} = \hat{C}_{i+\frac{1}{2}} + \mathrm{i}\omega\hat{A}^{-1}$ and $\underline{\hat{D}}'_{i+\frac{1}{2}}(x)$, $\underline{\hat{H}}'_{i+\frac{1}{2}}$ calculated with $\underline{\hat{C}}'_{i+\frac{1}{2}}$ instead of $\hat{C}_{i+\frac{1}{2}}$ the solution is in the interval $[x_i, x_{i+1}]$:

$$\begin{aligned}\underline{\vec{g}}(x)=&\ \mathrm{e}^{\underline{\hat{D}}'_{i+\frac{1}{2}}(x)}\left(\underline{\hat{H}}'_{i+\frac{1}{2}}\right)^{-1}\begin{pmatrix}\underline{\vec{g}}_{\mathrm{e},i}\\ \underline{\vec{g}}_{\mathrm{e},i+1}\end{pmatrix}\\&+\left[\underline{\hat{M}}_{i+\frac{1}{2}}(x)-\mathrm{e}^{\underline{\hat{D}}'_{i+\frac{1}{2}}(x)}\left(\underline{\hat{H}}'_{i+\frac{1}{2}}\right)^{-1}\begin{pmatrix}\hat{P}\underline{\hat{M}}_{i+\frac{1}{2}}(x_i)\\ \hat{P}\underline{\hat{M}}_{i+\frac{1}{2}}(x_{i+1})\end{pmatrix}\right]\\&\hat{H}^{-1}_{i+\frac{1}{2}}\begin{pmatrix}\vec{G}_{\mathrm{e},i}\\ \vec{G}_{\mathrm{e},i+1}\end{pmatrix}\underline{E}_{x,i+\frac{1}{2}}\end{aligned} \tag{9}$$

The matrix $\underline{\hat{M}}$ is given by an integral:

$$\underline{\hat{M}}_{i+\frac{1}{2}}(x)=\int_0^1\mathrm{e}^{\underline{\hat{D}}'_{i+\frac{1}{2}}(x)(1-\alpha)}\frac{\partial\hat{D}_{i+\frac{1}{2}}(x)}{\partial E_x}\mathrm{e}^{\hat{D}_{i+\frac{1}{2}}(x)\alpha}\mathrm{d}\alpha \tag{10}$$

The integral is evaluated by numerical means. Equation (9) can be used to build a linear system of equations for the even components of the small-signal solution similar to the dc case.

III. Simulation Results

A GaN HEMT similar to the one in Ref. [5] is investigated, where instead of 2000 gates only three are considered. The effective mass of the conduction band is $0.13m_0$, where m_0 is the free electron mass. The relative permittivity of GaN is 9.7, the temperature 300K and the surface recombination velocity $1.49 \cdot 10^7\mathrm{cm/s}$. A constant grid spacing of 10nm is used in transport direction ($N = 311$). The device is

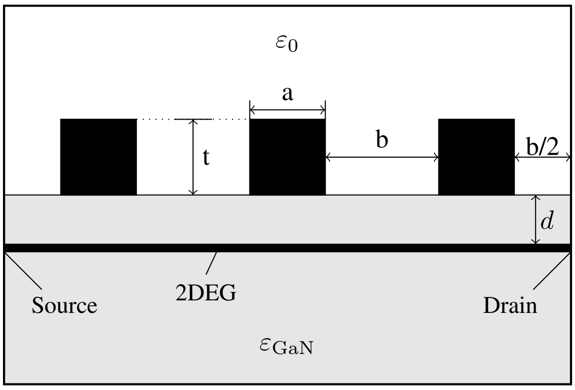

Fig. 1. HEMT with three gates and a 3μm long channel ($a = 0.34\mu$m, $b = 0.66\mu$m, $d = 0.026\mu$m, $t = 0.04\mu$m) [5].

simulated for the highest mobility mentioned in the paper ($4170\mathrm{cm}^2/\mathrm{Vs}$ and $\tau = 0.308$ps) (Fig. 2). The lowest order

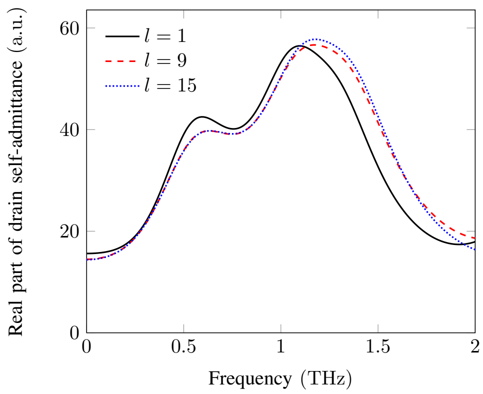

Fig. 2. Real part of the drain self-admittance ($\Re\{Y_{\mathrm{DD}}(j2\pi f)\}$) for $\mu = 4170\mathrm{cm}^2/\mathrm{Vs}$ and $V_{\mathrm{DS}} = 0$V.

model ($l = 1$) corresponds at zero drain/source bias to the model used by Dyakonov and Shur, since the (linearized) convective derivative is zero in this case. For this low mobility the expansion with Hermitian polynomials converges and reproduces the results of the BTE, which are not shown. In Fig. 3 the absolute value of the drain self-admittance is shown in the complex plane ($j\omega = \sigma + j2\pi f$) for $l = 1$. As expected, at a real part of $\sigma = -1/2\tau = -1.62/\mathrm{ps}$ a series of zeros and poles is found in accordance with the theory of Dyakonov and Shur [2]. The zeros (poles of the drain self-impedance) correspond to the plasma instabilities and they are strongly damped due to the low mobility and zero drain/source bias.

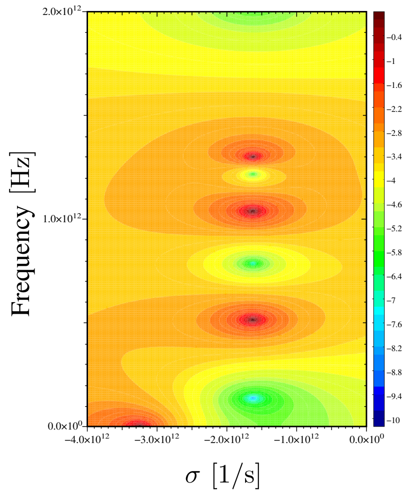

Fig. 3. Absolute value of the drain self-admittance ($|Y_{\mathrm{DD}}(\sigma + j2\pi f)|$) for $l = 1$, $\mu = 4170\mathrm{cm}^2/\mathrm{Vs}$ and $V_{\mathrm{DS}} = 0$V.

In the case of a model with 10 moments additional poles and zeros occur at about $\sigma = -1/\tau = -3.25/\mathrm{ps}$ (Fig. 4), which have negligible impact on the admittance at $\sigma = 0$ (Fig. 2). In

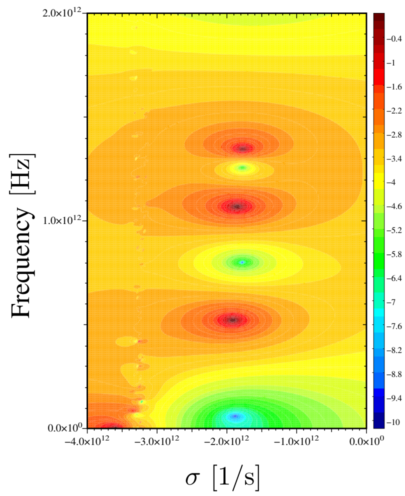

Fig. 4. Absolute value of the drain self-admittance for $l = 9$, $\mu = 4170\mathrm{cm}^2/\mathrm{Vs}$ and $V_{\mathrm{DS}} = 0$V.

Ref. [5] an electric field of 450V/cm was applied resulting in the case of three gates in a drain/source bias of $V_{\mathrm{DS}} = 0.135$V. As shown in Fig. 5 the results barely change and no negative real part of the drain self-admittance occurs. At such low mobilities THz waves cannot be generated and a much higher mobility with $2\pi f\tau \gg 1$ is required. In Fig. 6 results are shown for a 100 times higher mobility. The expansion with Hermitian polynomials no longer converges and the additional poles due to the higher moments (Fig. 7) have a much stronger impact on the drain self-admittance than in the case of the lower mobility (Fig. 4). Thus, the hydrodynamic model used by Dyakonov and Shur is not able to describe transport in devices with mobilities necessary for plasma oscillations even at zero drain/source bias. In the case of a nonzero bias the situation gets worse.

IV. Conclusions

Under quasi-ballistic conditions, the expansion with Hermitian polynomials no longer converges and plasma wave modeling requires a much more sophisticated transport model than the hydrodynamic model. Furthermore, it is not clear whether plasma instabilities can be used to generate THz waves with HEMTs.

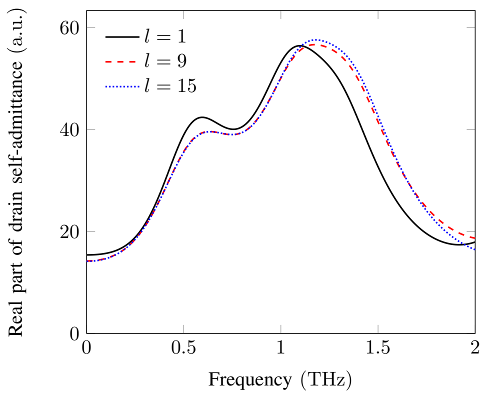

Fig. 5. Real part of the drain self-admittance for $\mu = 4170\mathrm{cm}^2/\mathrm{Vs}$ and $V_{\mathrm{DS}} = 0.135\mathrm{V}$.

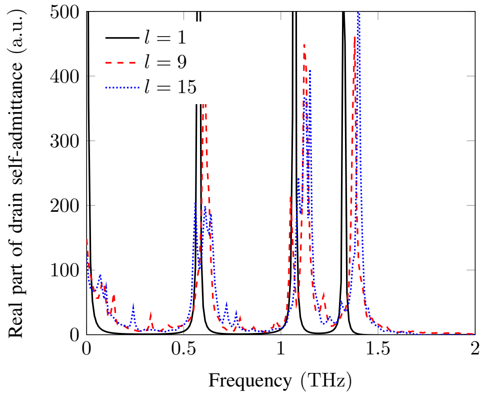

Fig. 6. Real part of the drain self-admittance for $\mu = 4.17 \cdot 10^5\mathrm{cm}^2/\mathrm{Vs}$ and $V_{\mathrm{DS}} = 0\mathrm{V}$.

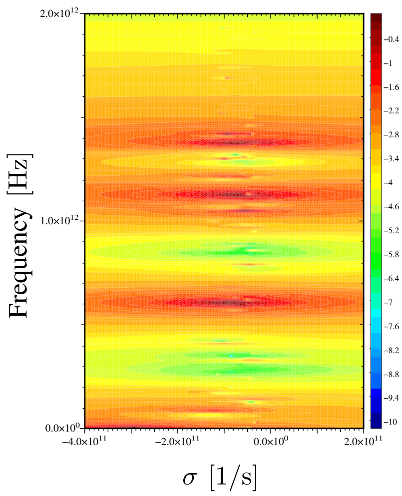

Fig. 7. Absolute value of the drain self-admittance for $l = 9$, $\mu = 4.17 \cdot 10^5\mathrm{cm}^2/\mathrm{Vs}$ and $V_{\mathrm{DS}} = 0\mathrm{V}$.

References

[1] T. Otsuji and M. Shur, "Terahertz plasmonics: Good results and great expectations," *Microwave Magazine, IEEE*, vol. 15, no. 7, pp. 43–50, Nov 2014.

[2] M. Dyakonov and M. Shur, "Shallow water analogy for a ballistic field effect transistor: New mechanism of plasma wave generation by dc current," *Phys. Rev. Lett.*, vol. 71, pp. 2465–2468, Oct 1993. [Online]. Available: http://link.aps.org/doi/10.1103/PhysRevLett.71.2465

[3] ——, "Plasma wave electronics: Novel terahertz devices using two dimensional electron fluid," *Electron Devices, IEEE Transactions on*, vol. 43, no. 10, pp. 1640–1645, Oct 1996.

[4] G. Gonzalez, *Microwave Transistor Amplifiers: Analysis and Design*, 2nd ed. Upper Saddle River, New Jersey: Prentice-Hall, 1997.

[5] V. Jakstas, I. Grigelionis, V. Janonis, G. Valusis, I. Kasalynas, G. Seniutinas, S. Juodkazis, P. Prystawko, and M. Leszczynski, "Electrically driven terahertz radiation of 2DEG plasmons in AlGaN/GaN structures at 110K temperature," *Applied Physics Letters*, vol. 110, no. 20, p. 202101, 2017. [Online]. Available: https://doi.org/10.1063/1.4983286

[6] Z. Kargar, T. Linn, D. Ruić, and C. Jungemann, "Investigation of transport modeling for plasma waves in THz devices," *IEEE Transactions on Electron Devices*, vol. 63, no. 11, pp. 4402–4408, Nov 2016.

[7] T. Grasser, T.-W. Tang, H. Kosina, and S. Selberherr, "A review of hydrodynamic and energy-transport models for semiconductor device simulation," *Proc. IEEE*, vol. 91, no. 2, pp. 251–274, 2003.

[8] T. Linn, Z. Kargar, and C. Jungemann, "Investigation of moments-based transport models applied to plasma waves and the Dyakonov–Shur instability," *Semiconductor Science and Technology*, vol. 34, no. 1, p. 014002, 2018.

[9] C. Jungemann, T. Grasser, B. Neinhüs, and B. Meinerzhagen, "Failure of moments-based transport models in nanoscale devices near equilibrium," *IEEE Trans. Electron Devices*, vol. 52, no. 11, pp. 2404–2408, 2005.

[10] N. Van Kampen, "The dispersion equation for plasma waves," *Physica*, vol. 23, no. 6-11, pp. 641–650, 1957.

[11] S. Selberherr, *Analysis and Simulation of Semiconductor Devices*. Wien: Springer, 1984.

[12] S.-M. Hong and J.-H. Jang, "Numerical simulation of plasma oscillation in 2-d electron gas using a periodic steady-state solver," *Electron Devices, IEEE Transactions on*, vol. 62, no. 12, pp. 4192–4198, Dec 2015.

[13] M. Abramowitz and I. A. Stegun, *Handbook of Mathematical Functions*. New York: Dover Publications, INC., 1972.

[14] H. Kim, H. S. Min, T. W. Tang, and Y. J. Park, "An extended proof of the Ramo-Shockley theorem," *Solid–State Electron.*, vol. 34, pp. 1251–1253, 1991.

[15] C. Moler and C. Van Loan, "Nineteen dubious ways to compute the exponential of a matrix, twenty-five years later," *SIAM review*, vol. 45, no. 1, pp. 3–49, 2003.

[16] D. L. Scharfetter and H. K. Gummel, "Large-signal analysis of a silicon read diode oscillator," *IEEE Trans. Electron Devices*, vol. ED-16, no. 1, pp. 64–77, 1969.